14th International Conference on Applications of Statistics and Probability in Civil Engineering, ICASP14
Dublin, Ireland, July 9-13, 2023

Uncertainty Quantification of Buckling Loads of Thin and Slender Structures Applying Linear and Nonlinear Analysis

Marc Fina
Chief Engineer, Institute for Structural Analysis, Karlsruhe Institute of Technology, Karlsruhe, Germany

Matthias G.R. Faes
Professor, Chair for Reliability Engineering, TU Dortmund University, Dortmund, Germany

Marcos A. Valdebenito
Chief Engineer, Chair for Reliability Engineering, TU Dortmund University, Dortmund, Germany

Werner Wagner
Professor, Institute for Structural Analysis, Karlsruhe Institute of Technology, Karlsruhe, Germany

Matteo Broggi
Chief Engineer, Institute for Risk and Reliability, Leibniz University Hannover, Hannover, Germany

Michael Beer
Professor, Institute for Risk and Reliability, Leibniz University Hannover, Hannover, Germany

Steffen Freitag
Professor, Institute for Structural Analysis, Karlsruhe Institute of Technology, Karlsruhe, Germany

ABSTRACT: Buckling is usually the governing failure mode for thin and slender structures. Small variations of geometrical or material parameters can have a major influence on the buckling behavior. Therefore, uncertainties have to be considered in a numerical buckling analysis which can be computationally expensive. In this paper, an approach to the estimation of the second-order statistics of the buckling loads is presented to reduce the computational effort. The second-order statistics are estimated by blending the results obtained from a linear and nonlinear buckling analysis by means of control variates. The approach is illustrated with a three-hinged arch and a cylindrical composite shell panel, where the input parameters are defined by random variables.

1. INTRODUCTION

The evaluation of the buckling load is a crucial issue when designing different types of structures. It is well known that buckling loads of structures are highly sensitive to random deviations from a nominal design, which may involve uncertainty regarding structural properties, geometry or boundary conditions (Broggi et al., 2011; Lauterbach et al., 2018). Hence, quantifying the level of uncertainties associated with buckling loads is a task of paramount importance (Fina et al., 2020, 2021). The buckling load can be approximated by means of a linearized approach (or linear buckling analysis), which involves the solution of an eigenvalue/eigenvector problem (see e.g. McGuire et al., 2000). While such an approach is quite convenient from a numerical point of view, it may offer limited insight due to its linearized nature. On the contrary, a nonlinear buckling analysis offers better prediction of the buckling load in case of a nonlinear prebuckling behavior. However, this requires a complete geometrically nonlinear path tracking analysis involving an iterative procedure. This means higher numerical costs compared to a linear buckling analysis. Considering these issues, this work aims to estimate the second-order statistics (mean and standard deviation) of buckling loads of thin and slender structures like frames and shells whose imperfections are characterized by means of probabilistic models. Some methods can only be used to estimate statistics for linear systems, see e.g. (Fina et al., 2023). The proposed approach is cast within the framework of control variates (Avramidis and Wilson, 1993). This allows to exploit correlations existing between buckling loads predicted using linear and nonlinear analysis. In fact, the more expensive analysis (that is, nonlinear approach) has to be done a few times only, while the cheaper analysis (that is, linearized approach) is used a considerable number of times. In this way, it is possible to estimate the statistics of the true buckling load, even when the linearized approach is involved in the analysis. In (Fina et al., 2022), the approach is first studied on an arch girder and one random variable. In the present paper, the approach is tested on a three-hinged arch and a composite cylindrical shell with up to four random variables. Thus, the correlation between the linear and nonlinear buckling analysis is investigated to show the applicability of control variates.

2. Basics of Buckling Analysis and Control Variates

2.1. *Linear and Nonlinear Buckling Analysis*

A stability point can be found using different strategies, as discussed, for example, in Wagner (1995). For some structures, it is possible to observe a linear prebuckling behavior. In such cases, a geometrical nonlinear analysis of the load-bearing behavior is not necessary and thus, only a single linear calculation step and solving an eigenvalue problem are required. This motivates to use the linear buckling analysis within a finite element (FE) model, which is based on the decomposition of the tangent stiffness matrix

$$\boldsymbol{K}_T = \boldsymbol{K}_{\text{lin}} + \boldsymbol{K}_{\text{nlin}} \quad , \tag{1}$$

where the stiffness matrix is divided into linear $\boldsymbol{K}_{\text{lin}}$ and nonlinear parts $\boldsymbol{K}_{\text{nlin}}$. Consequently, the eigenvalue problem for a linear buckling analysis can be constructed as follows

$$[\boldsymbol{K}_{\text{lin}} + \Lambda \boldsymbol{K}_{\text{nlin}}]\, \boldsymbol{\varphi} = \boldsymbol{0} \quad . \tag{2}$$

The linear buckling analysis assumes for the displacements $\boldsymbol{u} = \boldsymbol{0}$, where for an external load $\boldsymbol{P}_0$ the linear solution

$$\boldsymbol{K}_T(\boldsymbol{0})\boldsymbol{u}_0 = \boldsymbol{P}_0 \quad \Longleftrightarrow \quad \boldsymbol{u}_0 = \boldsymbol{K}_T^{-1}(\boldsymbol{0})\boldsymbol{P}_0 \tag{3}$$

is calculated with $\boldsymbol{K}_T(\boldsymbol{0}) = \boldsymbol{K}_{\text{lin}}$. The lowest eigenvalue Λ is used to increase the nonlinear parts of the stiffness matrix in the eigenvalue problem according Eq.(2). The associated eigenvector $\boldsymbol{\varphi}$ is called initial postbuckling mode. $\Lambda = 1$ leads to the mathematically precise eigenvalue problem

$$\boldsymbol{K}_T \boldsymbol{\varphi} = \boldsymbol{0} \quad . \tag{4}$$

In case of linear prebuckling behavior, it is assumed that

$$\boldsymbol{P}_{\text{cr}} \sim \Lambda \boldsymbol{K}_{\text{nlin}} \quad . \tag{5}$$

Solving the eigenvalue problem (2) leads to a critical load factor Λ_{cr}. The critical load with the corresponding critical displacement can be calculated by

$$\boldsymbol{P}_{cr} = \Lambda_{cr} \boldsymbol{P}_0 \quad , \tag{6}$$

$$\boldsymbol{u}_{cr} = \Lambda_{cr} \boldsymbol{u}_0 \quad . \tag{7}$$

In case of a nonlinear prebuckling behavior, the results of a linear buckling analysis can strongly differ from the correct buckling load. This requires a nonlinear buckling analysis, where a complete geometrically nonlinear path tracking analysis involving an iterative procedure by means of, e.g. the Newton-Raphson scheme, has to be performed. Parallel to the incremental calculation of the load-displacement behavior the diagonal signs of the tangent stiffness matrix can be observed. The sign of the diagonal elements of $\boldsymbol{K}_T$ determines the type of equilibrium state:

$$\begin{array}{llll} \forall D_{ii} & , & D_{ii} > 0 & \rightarrow \text{ stable} \\ \exists D_{ii} & , & D_{ii} = 0 & \rightarrow \text{ indifferent} \\ \exists D_{ii} & , & D_{ii} < 0 & \rightarrow \text{ unstable} \end{array} \quad . \tag{8}$$

If one or more diagonal elements D_{ii} become negative, an unstable equilibrium state is indicated Wagner (1995).

2.2. Control Variates

Thin and slender structures may be subject to variations of geometrical and material parameters. Such variations are represented through a vector $\boldsymbol{\xi}$ and hence, Eq. (1) becomes

$$\boldsymbol{K}_T(\boldsymbol{\xi}) = \boldsymbol{K}_{\text{lin}}(\boldsymbol{\xi}) + \boldsymbol{K}_{\text{nlin}}(\boldsymbol{\xi}) \tag{9}$$

It is assumed that uncertainty associated with $\boldsymbol{\xi}$ can be characterized in terms of a random variable vector $\boldsymbol{\Xi}$ with probability distribution $p_{\boldsymbol{\Xi}}(\boldsymbol{\xi})$ (Ditlevsen and Madsen, 1996). Given the uncertainty model associated with the imperfections, the buckling load $\boldsymbol{P}_{\text{cr}}$ also becomes uncertain. Such uncertainty can be expressed, for example, in terms of second-order statistics: mean $E[\boldsymbol{P}_{\text{cr}}]$ and variance $V[\boldsymbol{P}_{\text{cr}}]$. Given that there is no closed-form expression, which relates $\boldsymbol{P}_{\text{cr}}$ and $\boldsymbol{\xi}$, second-order statistics may be estimated by combining Monte Carlo simulation with nonlinear buckling analysis (Fishman, 1996), that is:

$$E[\boldsymbol{P}_{\text{cr}}] \approx \widehat{\mu_1'}(\boldsymbol{P}_{\text{cr}}, \boldsymbol{\Xi}_n) = \frac{1}{n}\sum_{j=1}^{n} \boldsymbol{P}_{\text{cr}}(\boldsymbol{\xi}^{(j)}), \quad \boldsymbol{\xi}^{(j)} \sim p_{\boldsymbol{\Xi}}(\boldsymbol{\xi}) \tag{10}$$

$$\begin{aligned} V[\boldsymbol{P}_{\text{cr}}] &\approx \widehat{\mu_2}(\boldsymbol{P}_{\text{cr}}, \boldsymbol{\Xi}_n) \\ &= \frac{1}{n-1}\sum_{j=1}^{n} (\boldsymbol{P}_{\text{cr}}(\boldsymbol{\xi}^{(j)}) - \widehat{\mu_1'}(\boldsymbol{P}_{\text{cr}}, \boldsymbol{\Xi}_n))^2 \quad , \\ &\text{with } \boldsymbol{\xi}^{(j)} \sim p_{\boldsymbol{\Xi}}(\boldsymbol{\xi}) \quad . \end{aligned} \tag{11}$$

In the above equations, $\boldsymbol{\Xi}_n$ represents n realizations of the random variable vector, that is, $\boldsymbol{\Xi}_n = [\boldsymbol{\xi}^{(1)}, \ldots, \boldsymbol{\xi}^{(n)}]$; $\boldsymbol{P}_{\text{cr}}(\boldsymbol{\xi}^{(j)})$ identifies the buckling load associated with the j-th realization of the imperfections $\boldsymbol{\xi}^{(j)}$; and $\widehat{\mu_1'}(\boldsymbol{P}_{\text{cr}}, \boldsymbol{\Xi}_n)$ and $\widehat{\mu_2}(\boldsymbol{P}_{\text{cr}}, \boldsymbol{\Xi}_n)$ represent estimators of the mean and variance of the buckling load $\boldsymbol{P}_{\text{cr}}$ as a function of the set of samples $\boldsymbol{\Xi}_n$. The application of Monte Carlo simulation for calculating second-order statistics of the buckling load is quite straightforward, as it can be carried out using existing numerical models for deterministic analysis. However, the calculation process itself may become quite demanding from a numerical viewpoint, as one may require a large number of analyses n to produce estimates of the second order statistics with sufficient accuracy. On top of that, each nonlinear buckling analysis can become quite involved on its own, due to the necessity of performing a Newton-Raphson iteration.

The estimation of second-order statistics can be improved by including results from the linearized buckling load $\hat{\boldsymbol{P}}_{\text{cr}}$ according to Eq. (2). In fact, calculating $\hat{\boldsymbol{P}}_{\text{cr}}$ is numerically cheaper than calculating the *exact* buckling load $\boldsymbol{P}_{\text{cr}}$. Although $\hat{\boldsymbol{P}}_{\text{cr}}$ is, in general, different from $\boldsymbol{P}_{\text{cr}}$, the framework of *control variates* (Fishman, 1996) can exploit correlations existing between these two bucking loads. Indeed, the mean of the buckling load μ_1' using control variates is equal to:

$$\mu_1' = E[\boldsymbol{P}_{\text{cr}}] - \alpha E[\hat{\boldsymbol{P}}_{\text{cr}}] + \alpha E[\hat{\boldsymbol{P}}_{\text{cr}}] \quad , \tag{12}$$

where α is the so-called control parameter, which is a real number. A close examination of Eq. (12) reveals that the expected value of the linearized buckling load $\hat{\boldsymbol{P}}_{\text{cr}}$ multiplied by the control parameter is added and substracted. Of course, from a theoretical viewpoint, the effect of this addition/substraction is zero. However, from a practical viewpoint, it is possible to exploit the correlation between $\boldsymbol{P}_{\mathrm{cr}}$ and $\hat{\boldsymbol{P}}_{\mathrm{cr}}$ as explained in the following. Let $\boldsymbol{\Xi}_n$ and $\boldsymbol{\Xi}_m$ be two independent sets of n and m samples of the random variable vector $\boldsymbol{\Xi}$, where $m > n$. Thus, the estimator of Eq. (12) becomes (Fishman, 1996):

$$\widehat{\mu_1'}^{(CV)} = \widehat{\mu_1'}(\boldsymbol{P}_{\mathrm{cr}}, \boldsymbol{\Xi}_n) - \alpha\widehat{\mu_1'}(\hat{\boldsymbol{P}}_{\mathrm{cr}}, \boldsymbol{\Xi}_n) + \alpha\widehat{\mu_1'}(\hat{\boldsymbol{P}}_{\mathrm{cr}}, \boldsymbol{\Xi}_m) \quad , \tag{13}$$

where the upper index *CV* denotes control variates. From this equation one observes the last term on the right (that is, $\alpha\widehat{\mu_1'}(\hat{\boldsymbol{P}}_{\mathrm{cr}}, \boldsymbol{\Xi}_m)$) is actually an estimator of the linearized buckling load calculated using m samples, which is multiplied by the control parameter α. As the linearized buckling load $\hat{\boldsymbol{P}}_{\mathrm{cr}}$ is numerically inexpensive to calculate (at least in comparison with $\boldsymbol{P}_{\mathrm{cr}}$), m can be relatively large in order to obtain an accurate estimator. The term $\widehat{\mu_1'}(\boldsymbol{P}_{\mathrm{cr}}, \boldsymbol{\Xi}_n) - \alpha\widehat{\mu_1'}(\hat{\boldsymbol{P}}_{\mathrm{cr}}, \boldsymbol{\Xi}_n)$ shown in Eq. (13) plays the role of *adjusting* the estimate of the mean value of the buckling load, as it computes the difference between the mean value of the *true* buckling load and the mean value of the linearized buckling load (the latter one amplified by α). As $\boldsymbol{P}_{\mathrm{cr}}$ and $\hat{\boldsymbol{P}}_{\mathrm{cr}}$ should exhibit a high correlation (because both characterize the buckling load), the variability of the estimator $\widehat{\mu_1'}(\boldsymbol{P}_{\mathrm{cr}}, \boldsymbol{\Xi}_n) - \alpha\widehat{\mu_1'}(\hat{\boldsymbol{P}}_{\mathrm{cr}}, \boldsymbol{\Xi}_n)$ should be low, even if n is relatively small. Thus, the control variates estimate as shown in Eq. (13) blends the information provided by both the linearized buckling load $\hat{\boldsymbol{P}}_{\mathrm{cr}}$ and the buckling load $\boldsymbol{P}_{\mathrm{cr}}$ to estimate the sought mean value.
The variance of the estimator for the mean as shown in Eq. (13) is (Fishman, 1996):

$$V\left[\widehat{\mu_1'}^{(CV)}\right] = \frac{\mu_{2,0}}{n} - 2\alpha\frac{\mu_{1,1}}{n} + \alpha^2\frac{\mu_{0,2}}{n} + \alpha^2\frac{\mu_{0,2}}{m} \quad . \tag{14}$$

Where $\mu_{p,q}$ is the bivariate central co-moment between $\boldsymbol{P}_{\mathrm{cr}}$ and $\hat{\boldsymbol{P}}_{\mathrm{cr}}$, which is defined as follows:

$$\mu_{p,q} = E[(\boldsymbol{P}_{\mathrm{cr}} - E[\boldsymbol{P}_{\mathrm{cr}}])^p(\hat{\boldsymbol{P}}_{\mathrm{cr}} - E[\hat{\boldsymbol{P}}_{\mathrm{cr}}])^q] \tag{15}$$

with p and q as the integers denoting the order of the respective co-moment. Unbiased estimators of these co-moments for different combinations of p and q can be found in, e.g. González et al. (2019). All of these co-moments can be calculated considering the sets of samples $\boldsymbol{\Xi}_n$ and $\boldsymbol{\Xi}_m$.
Eq. (14) indicates that the variance depends quadratically on the control parameter α. Thus, α is set such that the variance of the estimator of the mean is minimized, leading to the following expression

$$\alpha^* = \frac{\frac{\mu_{1,1}}{n}}{\frac{\mu_{0,2}}{n} + \frac{\mu_{0,2}}{m}} \quad . \tag{16}$$

The above discussion has been centered on the calculation of the mean value of the buckling load. Naturally, the same framework can be extended to calculate its variance. Following a similar strategy as that employed in Eq. (12), the variance μ_2 of the buckling load is:

$$\mu_2 = V[\boldsymbol{P}_{\mathrm{cr}}] - \gamma V[\hat{\boldsymbol{P}}_{\mathrm{cr}}] + \gamma V[\hat{\boldsymbol{P}}_{\mathrm{cr}}] \quad , \tag{17}$$

where γ is another control parameter. An estimate of the above equation can be calculated using the same set of samples generated for calculating the mean, yielding:

$$\widehat{\mu_2}^{(CV)} = \widehat{\mu_2}(\boldsymbol{P}_{\mathrm{cr}}, \boldsymbol{\Xi}_n) - \gamma\widehat{\mu_2}(\hat{\boldsymbol{P}}_{\mathrm{cr}}, \boldsymbol{\Xi}_n) + \gamma\widehat{\mu_2}(\hat{\boldsymbol{P}}_{\mathrm{cr}}, \boldsymbol{\Xi}_m) \quad . \tag{18}$$

The variance of the estimator of the variance is:

$$V\left[\widehat{\mu_2}^{(CV)}\right] = B_1 - 2\gamma B_2 + \gamma^2(B_3 + B_4) \quad , \quad , \tag{19}$$

where the terms B_1, B_2, B_3 and B_4 are defined as follows:

$$B_1 = V\left[\widehat{\mu_2}(\boldsymbol{P}_{\mathrm{cr}}, \boldsymbol{\Xi}_n)\right] = \frac{\mu_{4,0}}{n} - \frac{(n-3)\mu_{2,0}^2}{(n-1)n} \quad , \tag{20}$$

$$B_2 = \mathrm{Cov}\left[\widehat{\mu_2}(\boldsymbol{P}_{\mathrm{cr}}, \boldsymbol{\Xi}_n), \widehat{\mu_2}(\hat{\boldsymbol{P}}_{\mathrm{cr}}, \boldsymbol{\Xi}_n)\right] = \frac{2\mu_{1,1}^2}{(n-1)n} + \frac{\mu_{2,2}}{n} - \frac{\mu_{2,0}\mu_{0,2}}{n} \quad , \tag{21}$$

$$B_3 = V\left[\widehat{\mu_2}(\hat{\boldsymbol{P}}_{\mathrm{cr}}, \boldsymbol{\Xi}_n)\right] = \frac{\mu_{0,4}}{n} - \frac{(n-3)\mu_{0,2}^2}{(n-1)n} \quad , \tag{22}$$

$$B_4 = V\left[\widehat{\mu_2}(\hat{\boldsymbol{P}}_{\text{cr}}, \boldsymbol{\Xi}_m)\right] = \frac{\mu_{0,4}}{m} - \frac{(m-3)\mu_{0,2}^2}{(m-1)m} \quad . \tag{23}$$

Minimizing the expression for the variance in Eq. (19) provides a criterion for selecting the control parameter, leading to:

$$\gamma^* = \frac{B_2}{B_3 + B_4} \quad . \tag{24}$$

Note that for the practical calculation of Eqs. (20), (21), (22), (23), and (24), all required co-moments are estimated based on the sets of samples $\boldsymbol{\Xi}_n$ and $\boldsymbol{\Xi}_m$.

3. Numerical examples

The approach of control variates is illustrated on two buckling-sensitive structures. A three-hinged arch and a cylindrical composite shell panel under a single load is discussed. The input parameters are defined by random variables. Before the results of control variates are presented, the buckling behavior and the correlation between the linear and nonlinear buckling analysis are investigated.

3.1. *Three hinged arch*

The first example is a three-hinged arch subjected to a single load P at the middle hinge. The system is illustrated in Figure 1. The deterministic parameters are the length $L = 100\,cm$ and the cross section area $A = 25\,\text{cm}^2$. Overall, three uncertain parameters are modelled as truncated Gaussian random variables. Their mean value μ and standard deviation (std) σ are given in Table 1. The FE model consists of 20 nonlinear Timoshenko beam elements based on finite rotations with Green-Lagrangian strains. The load-displacement curves

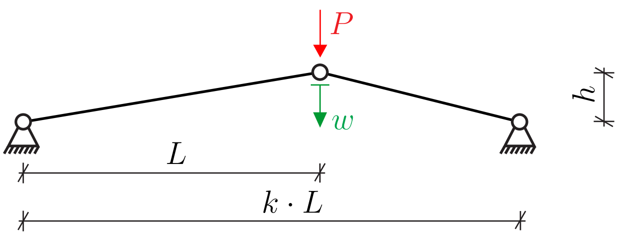

Figure 1: Three-hinged arch

Table 1: Material and geometrical parameters of the three-hinged arch quantified quantified as Gaussian random variables

Parameter	mean value μ	std σ
length factor $k\,[-]$	1.75	0.05
height $h\,[cm]$	$L/10$	$L/100$
Young's modulus $E\,[kN/cm^2]$	1000	100

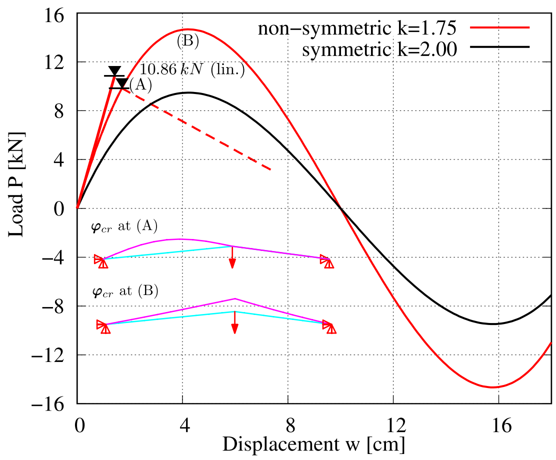

Figure 2: Load-displacement behavior of the three-hinged arch

for two different length factors $k = 1.75$ and $k = 2.0$ are depicted in Figure 2. The length factor k controls the symmetry of the system. A symmetric system results for $k = 2.0$ and a non-symmetric system for $k = 1.75$. This factor has a high influence on the buckling behavior. As shown in Figure 2, a non-symmetric ($k = 1.75$) three-hinged arch behaves more rigidly. Another interesting fact is that two types of stability points are present. Stability point (A) is a bifurcation point that can occur before the snap-through in point (B). In addition, the eigenvectors φ_{cr} associated with the two stability points are shown in Figure 2. The eigenvector φ_{cr} at the bifurcation point (A) represents a buckling of a single bar. The structure is loaded incrementally with the arc-length method and $\Delta w = 0.02\,cm$. Thus, a nonlinear buckling analysis gives the result of a critical load of $P_{cr} = 9.84\,kN$. A linear buckling analysis according to Eq. (2) leads to a critical load of $P_{cr} = 10.86\,kN$. Despite the large influence of the three input parameters on the buckling behavior, a strong correlation between linear and nonlinear buckling analysis can be observed, see Figure 3. These are good conditions for the application of control variates. In Table 2 the estimates for the second-order statistics are shown. The results obtained with the Monte Carlo simulation (see Eqs. (10) and (11)) and control variates approach (see Eqs. (13) and (18)) are given. In addition, Table 2 reports the coefficient of variation (δ) of each estimator, which is calculated as the square root of the variance of the estimator divided by its expected value. For Monte Carlo, the statistics are calculated considering $n = 100$ samples of the random parameters, each of which involves performing nonlinear buckling analysis. For control variates, one generates:

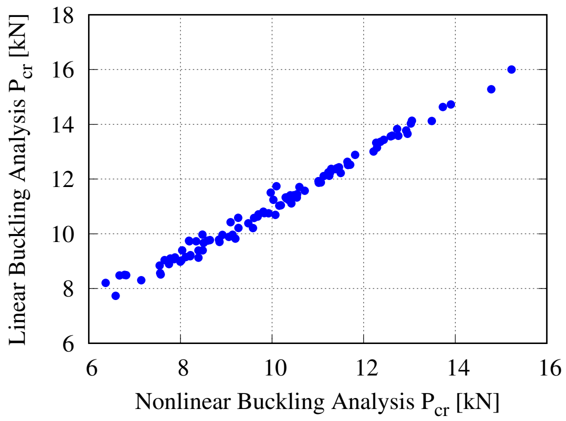

Figure 3: Correlation between linear and nonlinear buckling Analysis of the three hinged arch

Table 2: Estimates of second-order statistics for buckling load.

Approach	Monte Carlo	Control Variates with Splitting
n	100	60
m	0	90
n_e	100	97.5
$\widehat{\mu_1'}$ kN	10.05	10.04
$V\left[\widehat{\mu_1'}\right]$ kN^2	0.04	0.03
$\delta_{\widehat{\mu_1'}}$	1.96%	1.49%
$\widehat{\mu_2}$ kN^2	3.88	3.91
$V\left[\widehat{\mu_2}\right]$ kN^4	0.23	0.15
$\delta_{\widehat{\mu_2}}$	12.5%	8.96%

- $n = 60$ samples of the random parameter. For each of these 60 samples, buckling analyses considering both nonlinear and linearized equations are carried out.
- $m = 90$ additional samples. For each of these samples, only linear buckling analysis is carried out.

Numerical efforts between the two approaches are compared in terms of equivalent number of analyses n_e, that is:

$$n_e = n + \frac{n+m}{f_s} \tag{25}$$

where f_s is the speedup factor, which is the ratio between the time of execution of a nonlinear buckling analysis and a linear buckling analysis. For this particular example, $f_s = 4$ (that is, linear buckling analysis is 4 times faster than nonlinear buckling analysis). The results given in Table 2 indicate that the second-order statistics obtained when applying Monte Carlo simulation and control variates with splitting are almost identical. While numerical efforts are also similar (measured in terms of the equivalent number of analyses n_e), the estimates generated with control variates possess a smaller coefficient of variation than those associated with Monte Carlo. The latter is particularly notorious when comparing the coefficient of variation of the variance (that is, $\delta_{\widehat{\mu_2}}$) obtained through each method. In fact, if one would like to produce an estimate of the variance with a coefficient of variation as that one obtained with control variates but using Monte Carlo simulation, one would require to perform about 200 simulations (that is, perform 200 nonlinear buckling analyses). This is quite remarkable and highlights the advantages of the proposed framework considering control variates.

3.2. *Cylindrical composite shell panel under single load*

To show the approach for shell structures the second example is a composite shell under a single load similar as given in (Wagner and Gruttmann, 1994). The system with a 8×8 finite element mesh and the material data are shown in Figure 4. The shell is simply supported on the two lat-

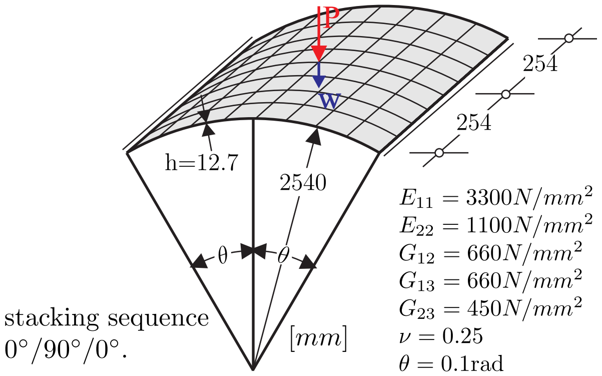

Figure 4: Cylindrical composite shell panel under a single load

eral edges. Symmetry is not used with respect to arbitrary stacking sequences and a parameter variation along the whole structure. In Figure 5 the load-displacement curves P versus w for three different shell thicknesses are depicted. The curves

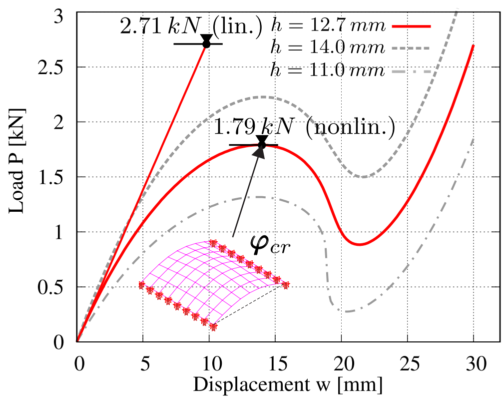

Figure 5: Load-displacement curves of the composite shell

are computed by the arc-length method. Even small variations of the shell thickness have a large influence on the buckling behavior. For a shell thickness of $h = 12.7\,mm$ a critical load of $P_{cr} = 1.79\,kN$ results from a nonlinear buckling analysis and a linear buckling analysis leads to a critical load of $P_{cr} = 2.71\,kN$. In Table 3, the defined truncated Gaussian random variables are listed. The given mean values and standard deviations are typical for a composite material. The variation of the fiber ori-

Table 3: Material and geometrical parameters of the cylindrical composite shell panel quantified as Gaussian random variables

Parameter	mean value μ	std σ
h	12.7	1.00
E_{11}	3300	330
E_{22}	1100	110
$\Delta\alpha$	0	1.50

entation α are considered within the stacking sequence: $0° + \Delta\alpha/90° + \Delta\alpha/0° + \Delta\alpha$. Figure 6 shows the correlations between linear and nonlinear buckling analysis for one parameter h (above) and all four parameters h, E_{11}, E_{22} and $\Delta\alpha$ (below) as random variables. If only h is defined as a ran-

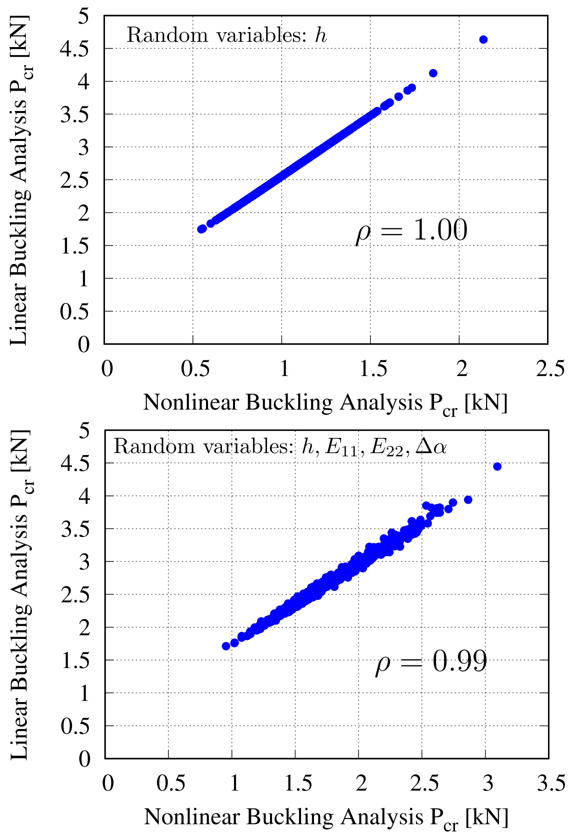

Figure 6: Correlations between linear and nonlinear buckling analysis of the composite shell

dom variable, a perfect correlation with correlation coefficient of $\rho = 1$ can be observed. More parameters defined as random variables do not significantly change the correlations. This is a good condition for using control variates. The results are given in

Table 4.

Table 4: Estimates of second-order statistics for the buckling load.

Approach	Monte Carlo	Control Variates with Splitting
n	500	60
m	0	555
n_e	500	375
$\widehat{\mu_1'}\ kN$	1.8	1.8
$V\left[\widehat{\mu_1'}\right]\ kN^2$	2.4×10^{-4}	2.3×10^{-4}
$\delta_{\widehat{\mu_1'}}$	0.9%	0.8%
$\widehat{\mu_2}\ kN^2$	0.121	0.125
$V\left[\widehat{\mu_2}\right]\ kN^4$	6×10^{-5}	6×10^{-5}
$\delta_{\widehat{\mu_2}}$	6.4%	6.3%

The mean and standard deviation are predicted nearly with the same precision (measured in terms of the coefficient of variation δ). However, the approach with control variates requires only a number of 375 equivalent simulations instead of 500.

4. CONCLUSIONS

The results presented in this contribution show a promising path for estimating second-order statistics of buckling loads. Indeed, blending the results of linearized and nonlinear buckling analyses, it is possible to obtain estimators with improved accuracy. However, the validity of the previous assertions must be thoroughly evaluated by addressing additional and more involved numerical models. In this paper, only random variables are used for the geometrical and material parameters. However, imperfections are spatially correlated. The applicability of the approach, when imperfections are modelled as random fields has to be investigated.

5. REFERENCES

Avramidis, A. and Wilson, J. (1993). "A splitting scheme for control variates." *Operations Research Letters*, 14(4), 187–198.

Broggi, M., Calvi, A., and Schuëller, G. (2011). "Reliability assessment of axially compressed composite cylindrical shells with random imperfections." *International Journal of Structural Stability and Dynamics*, 11(2), 215–236.

Ditlevsen, O. and Madsen, H. (1996). *Structural Reliability Methods*. John Wiley and Sons.

Fina, M., Faes, M., Valdebenito, M., Wagner, W., Broggi, M., Beer, M., and Freitag, S. (2022). "Estimation of second-order statistics of buckling loads applying linear and nonlinear analysis." *Proceedings of the 8th ISRERM*, M. Beer, E. Zio, K.-K. Phoon, and B. Ayyub, eds., Research Publishing.

Fina, M., Lauff, C., Faes, M., Valdebenito, M., Wagner, W., and Freitag, S. (2023). "Bounding imprecise failure probabilities in structural mechanics based on maximum standard deviation." *Structural Safety*, 101, 102293.

Fina, M., Panther, L., Weber, P., and Wagner, W. (2021). "Shell buckling with polymorphic uncertain surface imperfections and sensitivity analysis." *ASCE-ASME Journal of Risk and Uncertainty in Engineering Systems Part B: Mechanical Engineering*.

Fina, M., Weber, P., and Wagner, W. (2020). "Polymorphic uncertainty modeling for the simulation of geometric imperfections in probabilistic design of cylindrical shells." *Structural Safety*, 82, 101894.

Fishman, G. (1996). *Monte Carlo: concepts, algorithms and applications*. Springer, New York, NY.

González, I., Valdebenito, M., Correa, J., and Jensen, H. (2019). "Calculation of second order statistics of uncertain linear systems applying reduced order models." *Reliability Engineering & System Safety*, 190, 106514.

Lauterbach, S., Fina, M., and Wagner, W. (2018). "Influence of stochastic geometric imperfections on the load-carrying behaviour of thin-walled structures using constrained random fields." *Computational Mechanics*, 1–19.

McGuire, W., Gallagher, R., and Ziemian, R. (2000). *Matrix structural analysis*. John Wiley & Sons.

Wagner, W. (1995). "A note on FEM buckling analysis." *Communications in Numerical Methods in Engineering*, 11(2), 149–158.

Wagner, W. and Gruttmann, F. (1994). "A simple finite rotation formulation for composite shell elements." *Engineering Computations*, 11(2), 145–176.